

Supplementary Material

A study on the rules of ligands in highly efficient Ru-amide/AC catalysts for acetylene hydrochlorination

Yongwang Li^a, Fumin Wang^a, Jiaqi Hu^a, Mingshuai Sun^a, Jiawei Wang^a, Xubin Zhang^{a,*}

^aSchool of Chemical Engineering and Technology, Tianjin University, Tianjin 300350, P.R. China.

* Corresponding author: Xubin Zhang. E-mail address: tjzxb@tju.edu.cn.

Tel.: +86 22789041; fax: +86 22789041.

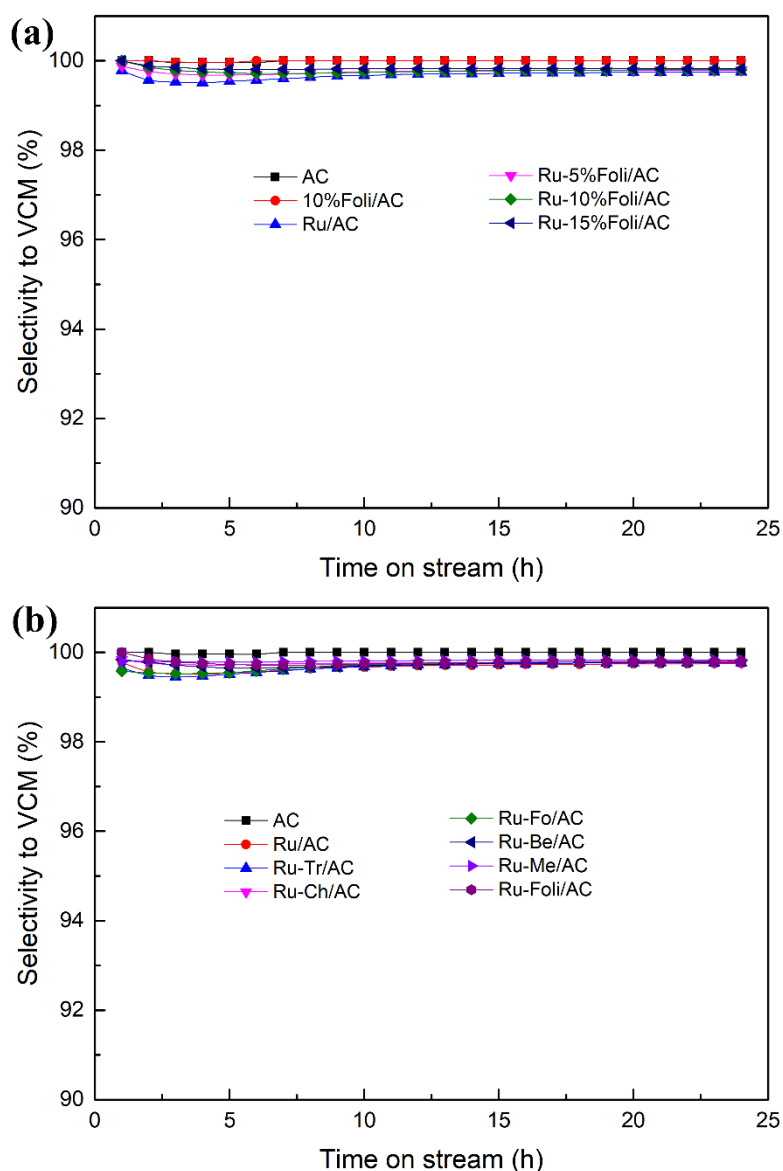


Fig. S1. VCM selectivity in acetylene hydrochlorination over (a) Ru-Foli/AC catalysts and (b) Ru-amide/AC catalysts. Reaction conditions: $T = 150\text{ }^{\circ}\text{C}$, $\text{GHSV}(\text{C}_2\text{H}_2) = 360\text{ h}^{-1}$, and $V_{\text{HCl}}/V_{\text{C}_2\text{H}_2} = 1.15$.

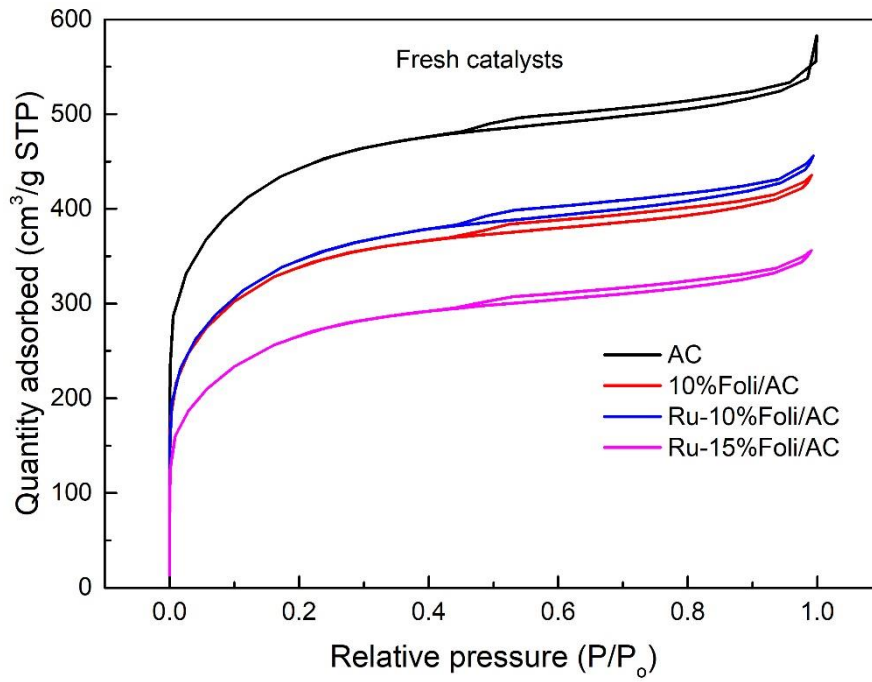


Fig. S2. N₂ adsorption-desorption isotherms of fresh catalysts

Table S1 The texture properties of fresh catalysts

Catalysts	S_{BET} (m ² ·g ⁻¹)	V_{p}^{d} (cm ³ ·g ⁻¹)
AC	1435.6	0.90
10%Foli/AC	1123.5	0.67
Ru-10%Foli/AC	1138.6	0.71
Ru-15%Foli/AC	897.48	0.55

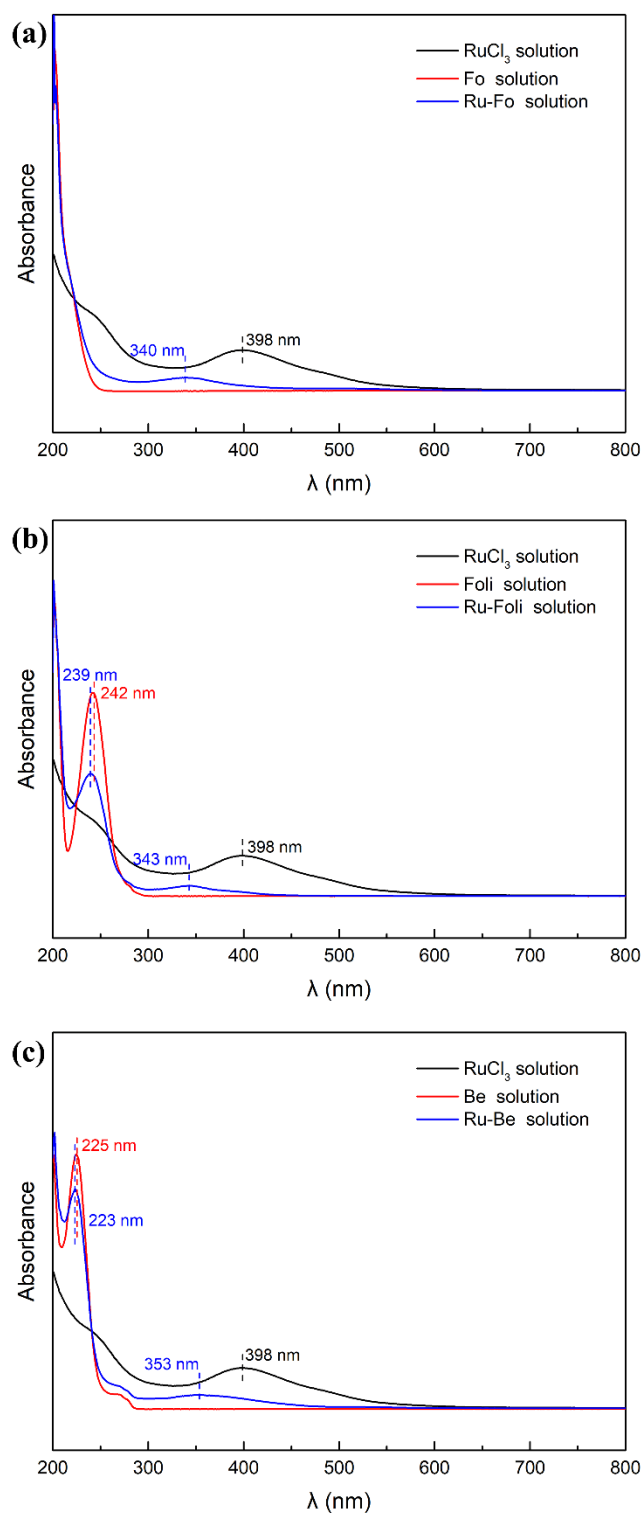


Fig. S3. UV-vis absorption spectroscopy of Ru, amide ligands, and Ru-amide ligands solution.

The UV-vis absorption spectroscopy of RuCl₃ solution shows a peak at 398 nm which corresponds to *d-d* transition of Ruⁿ⁺. As can be seen from Fig. S3(a), formamide shows no peak, while an absorption peak at 340 nm appears in the spectrum of Ru-Fo solution, which is the blue shift of the Ruⁿ⁺ peak. In Fig. S3(b), there is an absorption peak at 242 nm in the spectrum of formamide, which shifts to 239 nm in the spectrum

of Ru-Foli solution. Besides, the absorption peak of $\text{Ru}^{\text{n}+}$ in Ru-Foli solution also shifted to 343 nm. As for Fig. S3(c), same to Fig. S3(b), the absorption peaks of benzamide (from 225 to 223 nm) and $\text{Ru}^{\text{n}+}$ (from 398 to 353 nm) are blue-shifting. Because of the complexation between $\text{Ru}^{\text{n}+}$ and amide ligands, the charge transition requires more energy so that the absorption peak moves to the short wavelength.

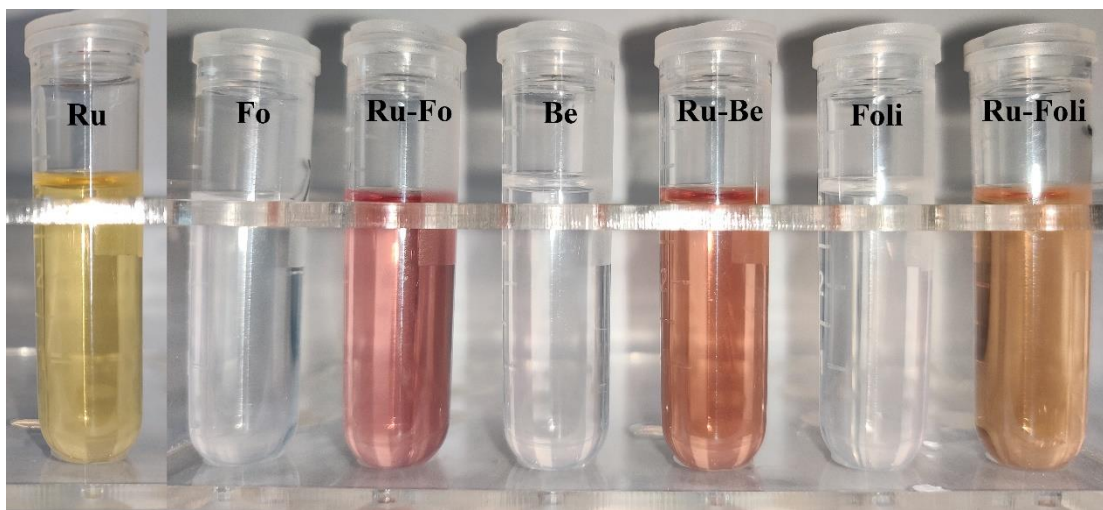


Fig. S4. Solutions of different samples.

RuCl_3 and amide ligands were dissolved in ethanol respectively, and Ru-amide solutions with the same ruthenium concentration as Ru solution were configured. It can be seen from Fig. S4 that the colors of Ru-amide solutions have changed compared with Ru solution, and the ligands themselves are colorless, which proves that the ligands may interact with ruthenium.

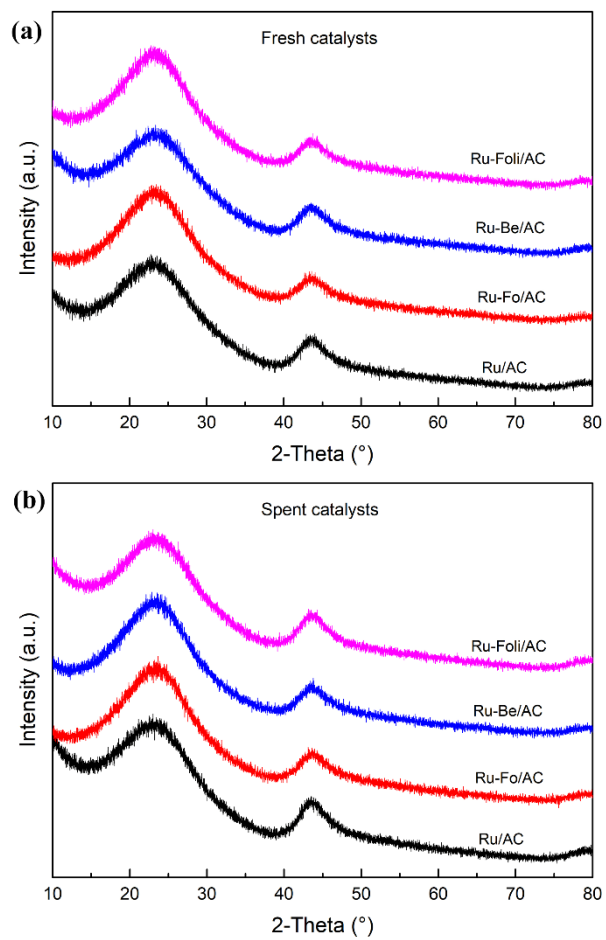


Fig. S5. XRD patterns of fresh and spent Ru-based catalysts.

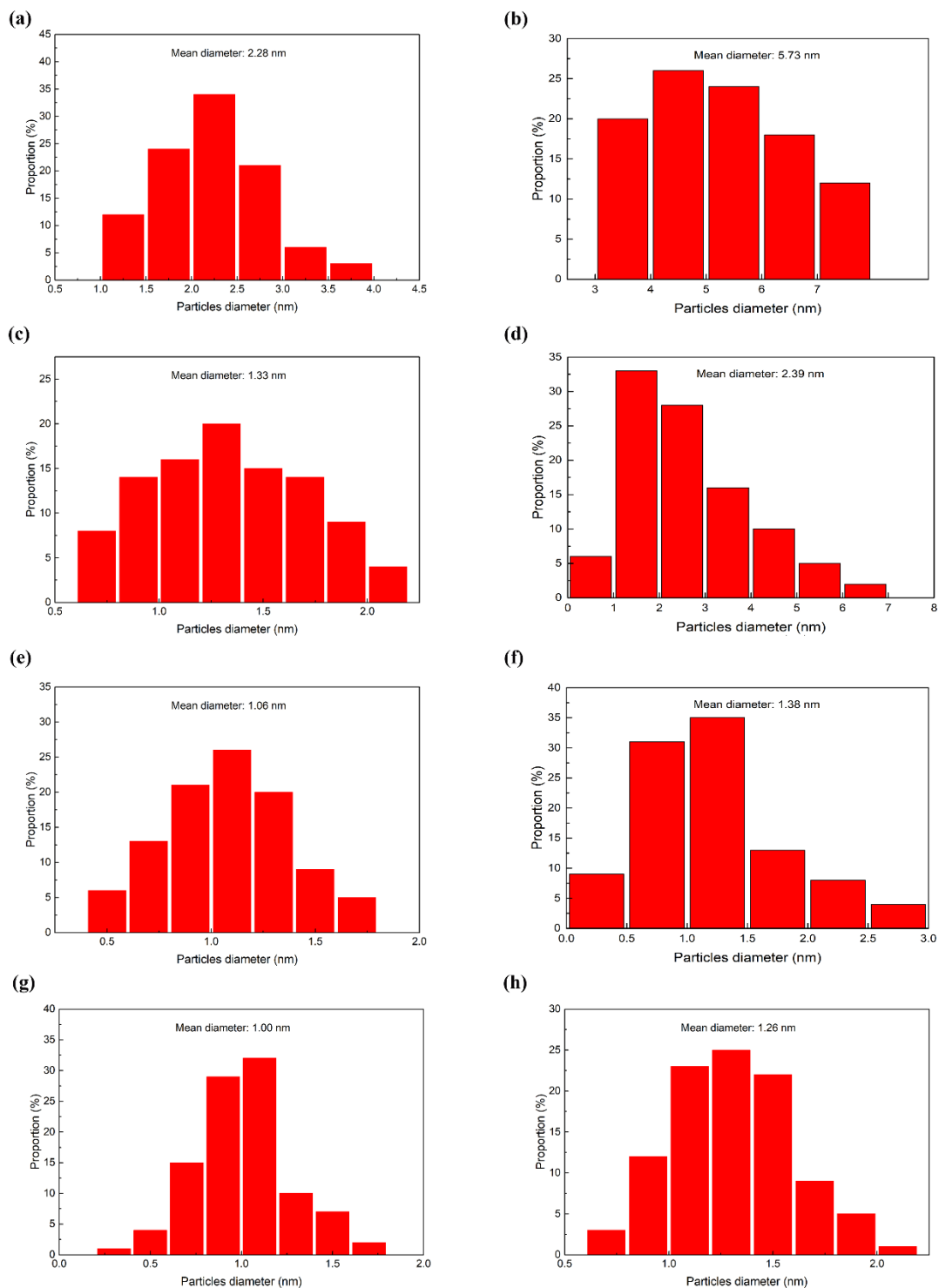


Fig. S6. Statistical data of particle size distribution of fresh and spent catalysts: (a) Fresh Ru/AC, (b) Spent Ru/AC, (c) Fresh Ru-Fo/AC, (d) Spent Ru-Fo/AC, (e) Fresh Ru-Be/AC, (f) Spent Ru-Be/AC, (g) Fresh Ru-Foli/AC, (h) Spent Ru-Foli/AC. (About 100 particles were measured for all samples.)

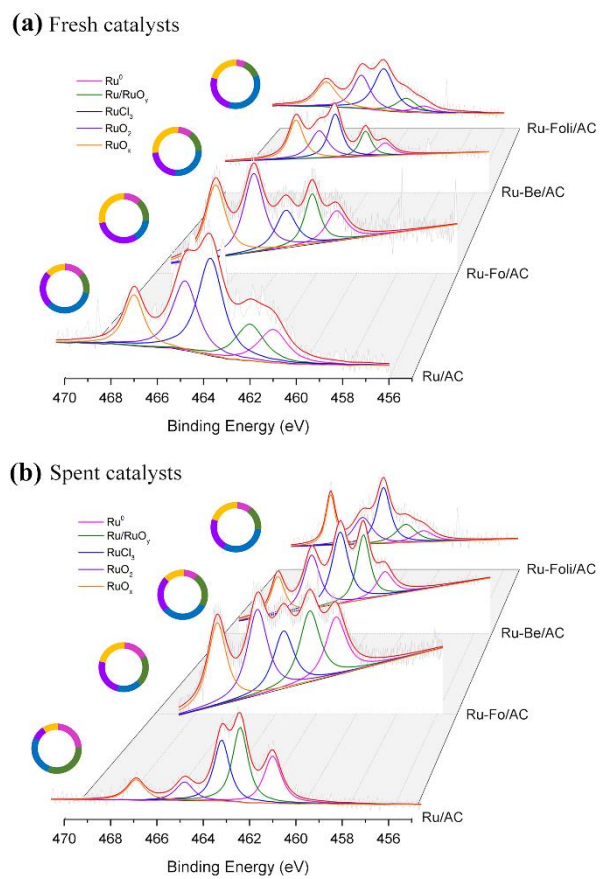


Fig. S7. XPS spectra of Ru 3p for fresh and spent Ru-based catalysts.

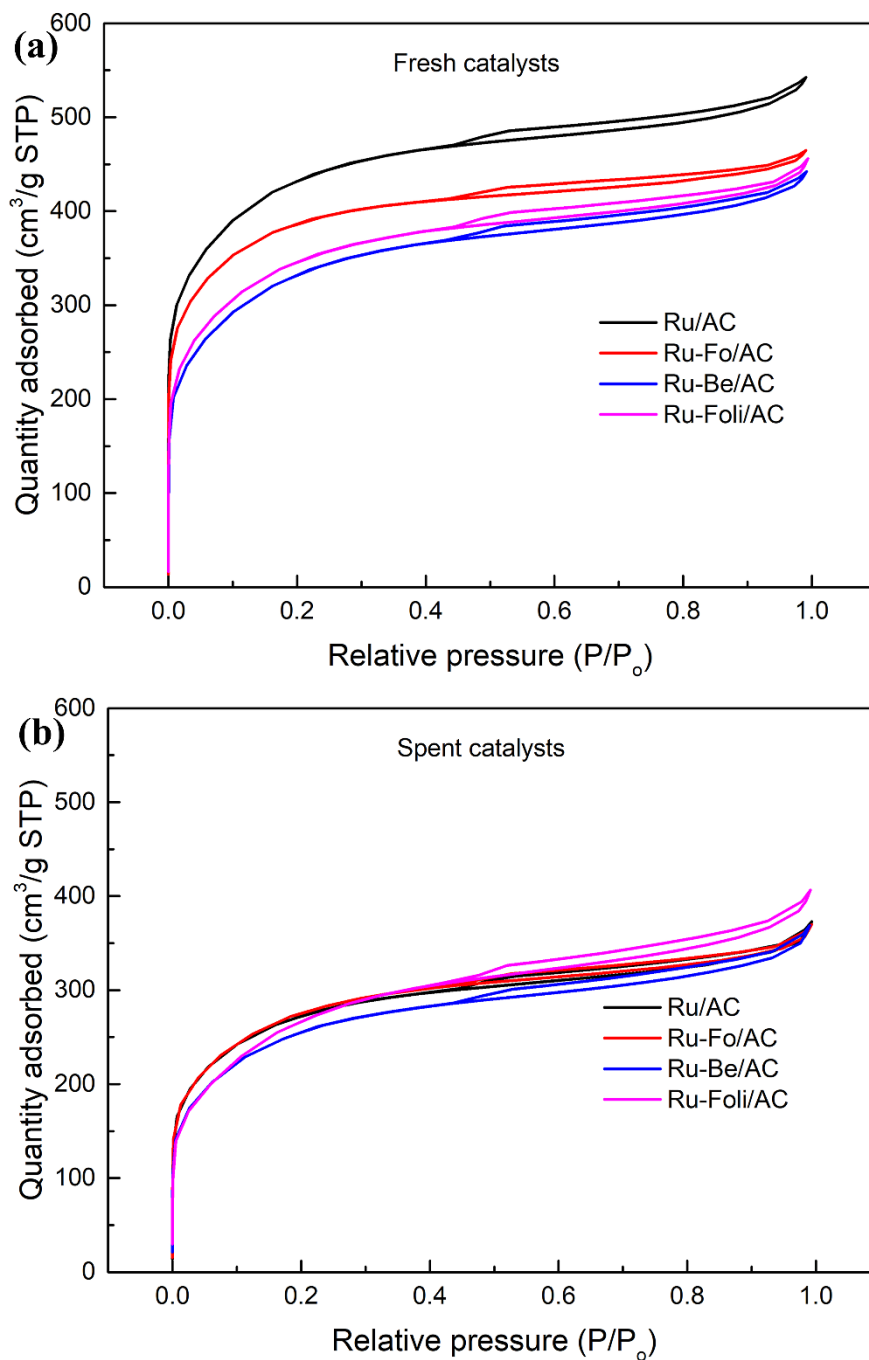


Fig. S8. N_2 adsorption-desorption isotherms of fresh and spent catalysts.

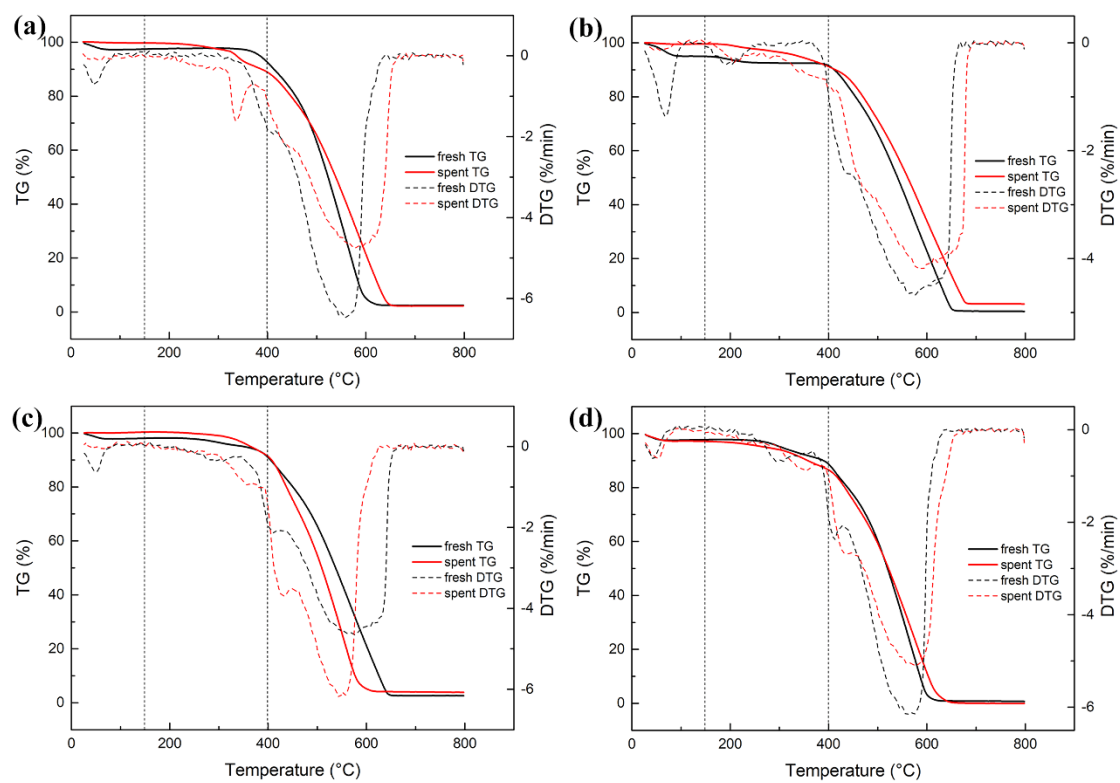
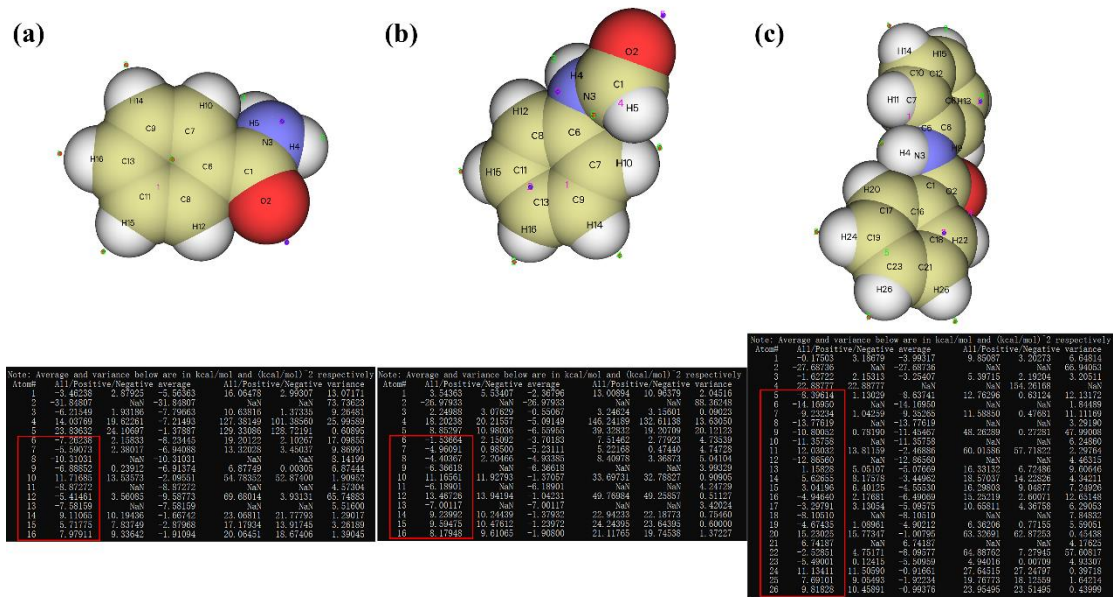


Fig. S9. TGA and DTG profiles of fresh and spent catalysts of (a) Ru/AC, (b) Ru-Fo/AC, (c) Ru-Be/AC and (d) Ru-Foli/AC.



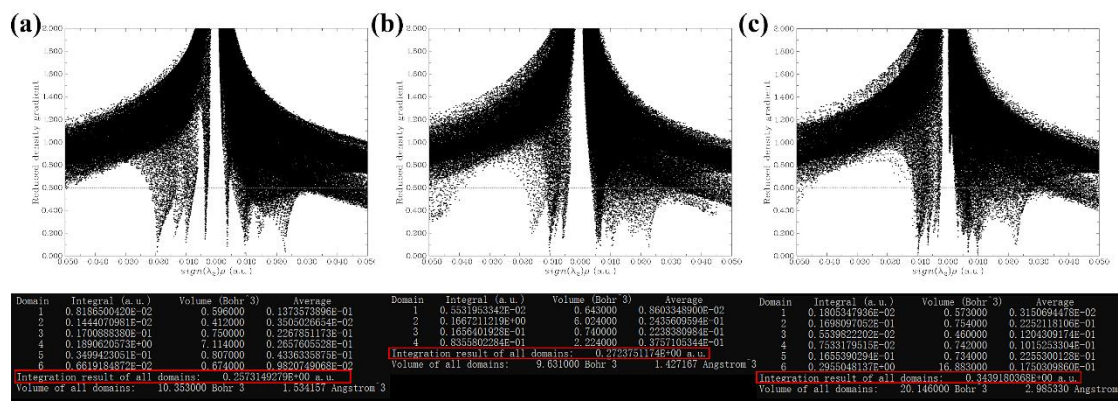


Fig. S11. Scatter graph of RDG function versus electron density multiplied and integration result of domains of (a) Ru-Be, (b) Ru-Foli, and (c) Ru-Beli.

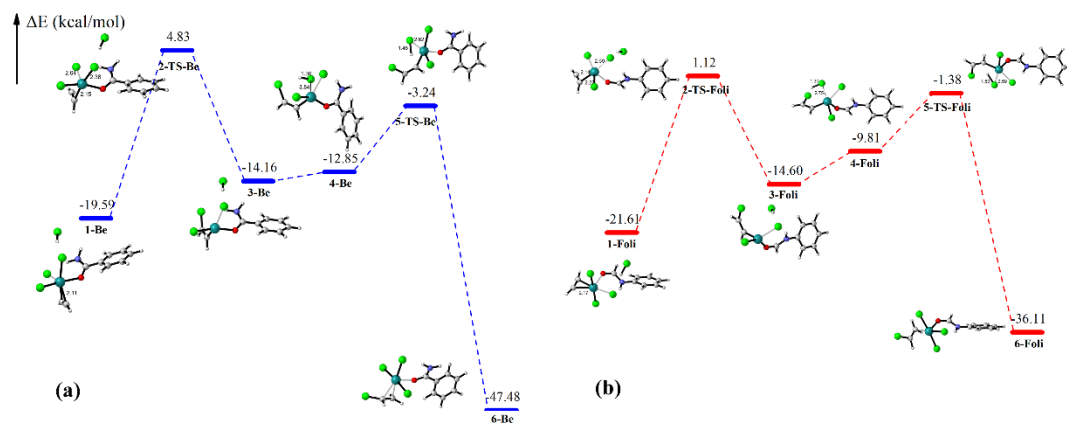


Fig. S12. Reaction paths of acetylene hydrochlorination over (a) Ru-Be/AC and (b) Ru-Foli/AC catalysts.

Table S2 Hirschfeld charge of RuCl₃ in Ru-Amide complexes

Ru-Amide complexes	Ru binding to O in amide ligands (e)	Ru binding to N in amide ligands (e)
Ru-Be	-0.25	-0.23
Ru-Foli	-0.26	-0.24
Ru-Beli	-0.30	-0.27

Table S3 Acetylene conversion over different Ru-based catalysts

Catalysts	Ru loading	Reaction condition	Acetylene conversion
Ru/AC-NHN ¹	1 wt%	180°C, 360h ⁻¹	93.2%
Ru1-Co3/SAC ²	1 wt%	170°C, 180h ⁻¹	95.0%
Ru/SAC-N700 ³	1 wt%	170°C, 180h ⁻¹	99.5%
Ru-in-CNT ⁴	1 wt%	170°C, 90h ⁻¹	99.1%
Ru/SAC-C300 ⁵	1 wt%	170°C, 180h ⁻¹	96.5%
Ru1K1/SAC ⁶	1 wt%	170°C, 180h ⁻¹	93.4%
Ru1Co3Cu1/SAC ⁷	0.1 wt%	170°C, 90h ⁻¹	99.3%
Ru-10%DMPU/AC ⁸	1 wt%	170°C, 900h ⁻¹	87.6%
1%Ru@15%TPPB/AC ⁹	1 wt%	170°C, 360h ⁻¹	99.7%
Ru-L ₁ /AC ¹⁰	1 wt%	180°C, 180h ⁻¹	96.5%
Ru-L ₈ /AC ¹⁰	1 wt%	180°C, 180h ⁻¹	99.0%
IPr-(Ru)/AC ¹¹	1 wt%	180°C, 180h ⁻¹	99.0%
Ru-Thi/AC ¹²	1 wt%	170°C, 400h ⁻¹	85.1%
0.5%Ru10%Foli/AC ^{This work}	0.5 wt%	160°C, 600h ⁻¹	89.1%
0.5%Ru10%Beli/AC ^{This work}	0.5 wt%	160°C, 600h ⁻¹	92.1%
0.2%Ru10%Beli/AC ^{This work}	0.2 wt%	160°C, 240h ⁻¹	95.1%

1. N. Xu, M. Zhu, J. Zhang, H. Zhang and B. Dai, *Rsc Advances*, 2015, **5**, 86172-86178.
2. J. Zhang, W. Sheng, C. Guo and W. Li, *Rsc Advances*, 2013, **3**, 21062-21068.
3. L. Hou, J. Zhang, Y. Pu and W. Li, *Rsc Advances*, 2016, **6**, 18026-18032.
4. G. Li, W. Li, H. Zhang, Y. Pu, M. Sun and J. Zhang, *Rsc Advances*, 2015, **5**, 9002-9008.
5. Y. Pu, J. Zhang, L. Yu, Y. Jin and W. Li, *Applied Catalysis a-General*, 2014, **488**, 28-36.
6. Y. Jin, G. Li, J. Zhang, Y. Pu and W. Li, *Rsc Advances*, 2015, **5**, 37774-37779.
7. H. Zhang, W. Li, Y. Jin, W. Sheng, M. Hui, X. Wang and J. Zhang, *Applied Catalysis B-Environmental*, 2016, **189**, 56-64.
8. H. Li, B. Wu, F. Wang and X. Zhang, *Chemcatchem*, 2018, **10**, 4090-4099.
9. S. Shang, W. Zhao, Y. Wang, X. Li, J. Zhang, Y. Han and W. Li, *Acs Catalysis*, 2017, **7**, 3510-3520.
10. J. Li, H. Zhang, M. Cai, L. Li, Y. Li, R. Zhao and J. Zhang, *Applied Catalysis A-General*, 2020, **592**, 117431.
11. M. Cai, H. Zhang, B. Man, J. Li, L. Li, Y. Li, D. Xie, R. Deng and J. Zhang, *Catalysis Science & Technology*, 2020, **10**, 3552-3560.
12. X. Wang, G. Lan, Z. Cheng, W. Han, H. Tang, H. Liu and Y. Li, *Chinese Journal of Catalysis*, 2020, **41**, 1683-1691.